Name: *Aly Khan Nuruddin* ***Student Number:*** *89444137*

Project Report – X-Ray Imaging

A. Introduction to X-Rays

Radiography is a medical imaging technique which involves bombarding a photographic plate with highly energetic, short frequency electrons generated within a vacuum tube. X-rays have a dual wave-photon nature like other characteristic emissions on the electromagnetic spectrum. The ionizing radiation transmitted through the patient's body following attenuation from the internal organs creates a neat, planar gray-scale 'projection' image which can be captured on the detector. The interaction of X-rays with matter is a function of energy, with higher absorptions occurring at greater wavelengths, which can be modulated by varying parameters such as the tube current, vacuum strength, as well as the applied voltage between the cathode and the anode (Bushberg, J. T et al, 2011).

B. Principles of X-ray Imaging

X-ray imaging utilizes principles of radiation physics, attenuation, and contrast resulting in differential absorption of by various tissues or materials to produce diagnostic images. After the X-rays are produced by accelerating electrons in a glass tube towards a metal target (usually tungsten), they pass through the body or object being imaged. Dense materials (such as bone or metal) can absorb more X-rays, causing attenuation and fewer X-rays reaching the detector while less dense materials (such as soft tissue) allow more X-rays to pass through. Due to image contrast, bones appear white on the image, while soft tissues appear in shades of gray and air-filled organs such as lungs, appear darker. The detector captures the image producing 2D projection of a 3D object along with image resolution. Image quality is optimized by balancing contrast, resolution, noise, and the presence of any artifacts. To ensure patient safety, minimum radiation dose, controlled exposure time, proper positioning and lead shielding are often used (Harvey CJ, 2008).

C. X-Rays for Chest Imaging

X-rays are commonly utilized to image the chest and thoracic cavity, usually requiring an applied voltage of 120kV, which corresponds to the same equivalent photon energy with units of keV. As a diagnostic tool, X-rays are inexpensive, non-invasive, and highly effective in delineating and detailing structures within the chest including lungs, heart, vasculature, and bones, amongst others. Radiologists can glean valuable information about the state of the patient's internal organs from output X-ray images, which can correspondingly be used to identify abnormalities, characterize medical conditions, and inform treatment options for the disease or infection. X-rays are particularly well-suited for visualization of the lungs due to the high contrast achievable between air and soft tissue. This corresponds to the stark difference in attenuation amongst the two materials, with the former (air) absorbing fewer photons compared to the latter (soft tissue) (Niederman, M. S et al, 2008).

D. Radiology Diagnoses for Lung Infections

The current state-of-the-art procedure for diagnosing lung infections involves examining subtle differences between images obtained for normal and viral subjects. A healthy, well-functioning pair of lungs is denoted by plenty of dark pixels, appearing radiolucent due to the greater volume of air present. Further, normal vascular markings are observed, especially near the hila which taper off toward the lung periphery. Other features include sharp diaphragm margins, cardiac silhouette, midline trachea and bronchi with no pleural fluid (Rosa, M. E et al, 2018).

On the other hand, infected lungs are dotted with deformities and underlined by specific characteristics such as consolidation, ground-glass opacities or nodules. Consolidation is a prominent sign of pneumonia and corresponds to a cloudy, white region within air-filled spaces due to infiltration of fluid, pus or some other

infectious material. Additionally, ground-glass opacities are lighter, hazy areas on X-ray projections that indicate partial displacement of air in the lung with fluid. This feature is considered a common hallmark of viral diseases such as COVID-19 and is often seen bilaterally in lower lobes of the lung as well as peripherally. In Influenza, the bilateral reticular infiltrates present as patchy ground-glass opacities. Similarly, RSV (Respiratory Syncytial Virus) infection is characterized by peribronchial thickening and patchy opacities. Lastly, rounder nodules or masses specify the eminence of highly local, pus-filled papules with an opaque image gradient that correspond to the presence of abscesses in the lung.

In contrast to bacterial infection, viral infection presents more diffusely, with a lack of localized or lobar consolidation. Instead, it is distinguished by absence of pleural effusion (buildup of fluid in the space between the lungs and the chest wall), which results in blunting of costophrenic angle. In some viral infections like bronchiolitis, the lungs may show signs of hyperinflation due to overinflation with air, as well as flattened diaphragms and increased spacing between the ribs. Areas of partial lung collapse or atelectasis appear as regions of increased density, along with shifts of mediastinal structures like the heart or trachea. Advanced infection in the form of lung abscess may be complicated by the presence of additional features like cavitation, which is a hollowed-out area within a dense, consolidated region. In patients with underlying lung diseases and chronic smokers, destruction of the tissue may occur as large dark spaces called emphysema.

E. Limitations of Manual Radiology Diagnoses

Presently, radiologists often manually diagnose viral diseases such as COVID-19 by the presence of airspace opacities indicative of infection. However, interpreting chest X-rays is a complex and challenging task, which requires specialized expertise and training for correctly identifying subtle abnormalities. Due to the planar, 2D nature of X-rays, structures like ribs, blood vessels, and soft tissues overlap frequently, thereby obscuring small lesions. X-rays have limited depth perception and so provide a flat image of a three-dimensional structure. Sometimes the suboptimal image quality can significantly complicate the clinical interpretation process (Chockalingam, S et al, 2019).

To make a comprehensive diagnosis, X-ray findings are required to be interpreted in the light of patient's symptoms (such as fever, cough and shortness of breath), relevant physical examination findings, and lab tests such as white blood cell count and sputum cultures. Comparison of recent X-ray images with previous ones becomes quite helpful in determining whether the infection is progressing, resolving, or stable. Hence, supplementing chest X-rays with advanced imaging techniques through other modalities like CT and MRI, with AI-powered tools could remarkably improve diagnostic accuracy and comprehensiveness, especially during the early-stage of lung diseases, as well as in characterizing fine ground-glass opacities of viral infections.

F. Artificial Intelligence for Computational Diagnoses

The implementation of computer-aided solutions provides an alternative for efficient diagnosis of X-ray images by considerably reducing human error and effort. Software engineers, in collaboration with data scientists and medical professionals, can process and transform raw image data-stores into formats such as NIFTI or DICOM, which are suitable for deep learning algorithms, while facilitating accurate analysis of patterns, segmentation and classification (Meedeniya, D et al, 2022).

Convolutional Neural Networks (CNNs) is a popular deep learning technique for medical image classification capable of dissecting complex image features, while requiring relatively fewer parameters and possessing the advantage of weight-sharing. Based on dataset quality, model architecture, and applied pre-processing techniques, the accuracy of CNNs may vary from 83% to 96%. New methods for diagnosing COVID-19 using

CNNs are continually emerging and is an active area of research in medical imaging. In a recent study by Padma and Kumari [41], a CNN built from scratch, consisting of convolutional and max-pooling layers followed by fully connected kernels, achieved an impressive accuracy of 98.3%.

Another Deep Learning technique for classification of chest radiography images is transfer learning, which considers translationally relaying knowledge across attention networks to improve model performance while reducing learning costs. Irfan et al. [23] used pre-trained models on ResNet-50, InceptionV3, and DenseNet121 for classification of pneumonia using chest X-ray images, achieving higher accuracy compared to models trained from scratch.

Two forms of transfer learning are commonly used in chest X-ray image analysis: feature extraction and fine-tuning. The former consists of convolutional layers corresponding to the pre-trained model (e.g., ResNet, DenseNet) from large datasets like ImageNet, which are applied directly to the chest X-ray images. The final, fully connected layer is then refined or replaced to adapt to the new task of classifying chest X-rays, often for identifying lung infections such as pneumonia or COVID-19. Meanwhile, fine-tuning comprises of a pre-trained model which utilizes both feature extraction and refinement throughout the network. This allows for greater specialization of the model to the medical task and sufficiently improves performance in the presence of adequate labeled data. As an example, through combination of feature-extraction and fine-tuning, the VGG-16 based model achieved a higher accuracy of 98.3%.

Despite its advantages, transfer learning has several potential disadvantages such as domain mismatch, overfitting and higher computational costs, especially when adjusting for multiple layers or large architectures. Moreover, there is limited control over extracted features from source task.

Therefore, to improve the accuracy and robustness of the model, ensemble classification is used to combine multiple configurations like bagging (e.g., Random Forests), boosting (e.g. AdaBoost, XGBoost), or stacking. By aggregating predictions from various models such as decision trees, neural networks, or support vector machines, the ensemble reduces potential errors of individual models, making the combined outputs' reliability as high as 99.87%.

Image segmentation is another possible technique of enhancing diagnostic accuracy within medical imaging. Through focused analysis, it allows radiologists to concentrate on relevant anatomical areas while allowing for improved extraction of features such as size, shape, and texture. By isolating structures of interest, segmentation helps reduce the impact of background noise or irrelevant information in the image, leading to clearer and more interpretable results.

G. Principles of Image Analysis

The decision-making steps during image analysis involve the systematic examination and interpretation of visual data through various techniques. During image acquisition, first the raw images are captured. This is followed by preprocessing by correcting noise, contrast, or brightness, to enhance the image quality. After the image editing through binary processing, segmentation divides the image into meaningful regions or objects for focused analysis. Through feature extraction, characteristics like edges, shapes, textures, or colors are identified and quantified. Pattern recognition or machine learning provide classification for interpretation and decision making. Finally, findings are refined through post-processing and accuracy is enhanced by comparing outputs with the expected outcomes (Grande JC, 2012).

H. Metrics of Image Quality

Image quality can be assessed quantitatively through several key parameters. The better image quality is reflected by higher Peak Signal-to-Noise Ratio (PSNR) and Structural Similarity Index (SSIM) of 1. On the other hand, lower Mean Squared Error (MSE) and higher Contrast-to-Noise Ratio (CNR) and higher entropy values indicate greater better quality. Similarly, a higher Modulation Transfer Function (MTF) and a higher Signal-to-Noise Ratio (SNR) are indicative of better sharpness and resolution. Other parameters of image quality are edge-sharpness and color accuracy (Umme Sara et al, 2019).

I. Exploratory Analysis of X-Ray Images

The attenuation of lung tissue under normal and infected states can be utilized to characterize patients into diseased and healthy groups. Due to the fuzziness generated within the lungs in infected patients from the buildup of viral pathogens in the pleural cavity, a number of imaging metrics such as resolution, contrast, and signal-to-noise ratio, can be affected. However, in both instances, artifacts from repeated motion, underexposure or overexposure of photographic film, improper positioning, grid misalignment, and aliasing, amongst others, can significantly hinder the image quality, and consequently the accuracy of the diagnosis. Image resolution corresponds to the amount of detail captured, which can be significantly impaired by blurriness induced in viral infections from interstitial patterns. However, well-defined consolidation in the case of bacterial infections allows for less obstruction and greater visibility of internal chest structures. Meanwhile, contrast is another prominent metric that seeks to quantify relative differences between adjacent regions of an image. Similarly, an increase in lung opacity for viral infections reduces contrast while more obtuse conformations for bacterial infections enhances contrast, in comparison, making it easier to identify from X-ray images of the chest. The quality of the image is often characterized by a high signal-to-noise ratio (SNR), which increases with the square of the signal strength as a function of spatial frequency. Although an optimal SNR is integral for creating an appropriate map of attenuation coefficients, there is always a tradeoff with dose.

Alternatively, a histogram analysis can be conducted to plot the image intensity displayed on screen with the intensity in memory, by ‘binning’ the pixels according to their gray-scale values. Based on our knowledge of the biological changes that arise in the pleural cavity for infectious diseases, it can be hypothesized that the number of brighter (white) pixels would be greater for lungs with viral load compared to healthy lungs, which would tend to have a higher number of darker (black) pixels due to a larger volume of air in the tracheobronchial tree and alveolar sacs.

Additionally, from linear systems theory, specific kernels or filters can be applied to highlight relevant regions of interest within the image. A popular derivative operator is the Sobel filter, which uses integer elements and can be implemented as a weighted average for the Laplacian. The kernel, which corresponds to the double-derivative of the Gaussian, is good for emphasizing edges in both the x and y-axes. This can be extremely beneficial in performing segmentation of the image for identification of pixels corresponding to higher intensities, and thus the infected load within the patient. The images obtained for the analyses were provided in the assignment description and extracted from the open-source repository, *Mendeley Data*.

J. X-Ray Image Analyses

The following histogram plots were obtained in MATLAB for both normal and infected lung images, provided in Kermany, Daniel S. et al. (2017), with the code given. (Figure #1)

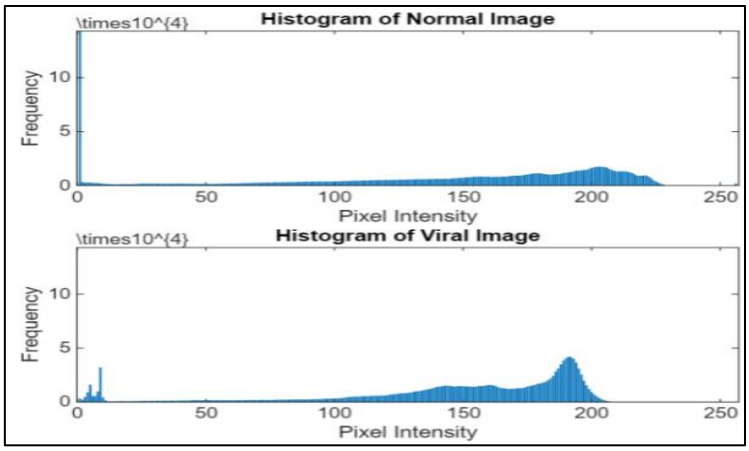

Figure #1: *Histogram Plots of Normal & Viral Images.*

As can be seen in the above graph for the normal image, there is a huge spike corresponding to the pixel intensity for 0, followed by fewer gray-scale values and a few thousand brighter pixel intensities between 175 and 225. On the other hand, the plot for the viral image is characterized by two peaks, one at a pixel value of 10 and another at 190. In contrast to the chest X-ray scan for the normal lungs, there is a sizeable chunk of brighter pixels and an equivalent depreciation in the number of darker pixels. This aligns well with our hypothesis and is indicative of the changes in pixel intensities for images related to normal and viral lung infections, respectively. Moreover, the differences between histograms can be attributed to the greater amount of blurring observed in the viral load image, due to a higher volume of fluid or pus in lungs instead of air. The features mentioned previously, including ground-glass obscurities, alveolar consolidations, infiltrates and nodules, could be prominent within the lungs with the viral infection.

Meanwhile, the Sobel filter for edge detection implemented in MATLAB, yielded the following results for both normal and viral images, with the code documented for reference (Figure #2).

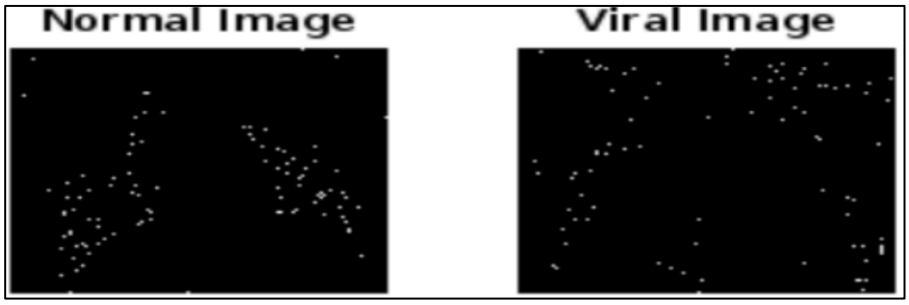

Figure #2: *Sobel Edge Detection Filter for Normal & Viral Images.*

The observed white spots in both images correspond to the edges in the x and y-directions, as indicated by the edge detection algorithm in MATLAB. For the normal image, the outlines of the two lungs are clearly demarcated, whereas for the viral image, the dots are sparsely scattered on the periphery. This suggests that the computer program struggled with accurately delineating the borders for the viral image, primarily due to poor contrast and lack of sharpness around the edges. On the contrary, a faint marking of the heart and diaphragm is also visible within the image for normal lungs, indicating greater success of the algorithm in extracting the edges. Once again, the difference between the two images can be assigned to the induced blurriness due to infiltration of the viral load within the lungs, which induces artifacts and makes it challenging for the software, along with the radiologists as seen previously, to detect the appropriate edges.

K. Conclusion

The following report summarized the findings highlighted in literature for quantifying differences between normal and viral chest X-ray images, both from a clinical and engineering perspective. Further, the report outlined different characteristic, visual elements of infectious lung diseases and highlighted possible machine learning alternatives for sharpening image features. Lastly, the document showcased results from preliminary processing methods such as histograms and Sobel edge detection, to verify outcomes from a radiology point of view.

References:

Bushberg, J. T., Seibert, J. A., Leidholdt, E. M., & Boone, J. M. (2011). *The essential physics of medical imaging* (3rd ed.). Lippincott Williams & Wilkins

Chockalingam, S., Hong, K., & Donmez, M. (2019). Limitations of manual interpretation in radiology: Improving diagnostic accuracy with computer-aided detection. *Journal of Digital Imaging, 32*(5), 720-728. https://doi.org/10.1007/s10278-019-00237-6.

Grande, J. C. (2012). The expanding role of radiology in global health. *Radiologia Brasileira, 45*(3), 175-181. https://doi.org/10.1007/s13632-012-0037-5

Harvey, C. J. (2008). The principles of X-ray imaging. *Clinical Radiology, 63*(5), 491-495. https://doi.org/10.1016/j.crad.2008.01.007

Meedeniya, D., Kumarasinghe, H., Kolonne, S., Fernando, C., Díez, I. T., & Marques, G. (2022). Chest X-ray analysis empowered with deep learning: A systematic review. *Applied Soft Computing, 126*, 109319. https://doi.org/10.1016/j.asoc.2022.109319

Niederman, M. S., & Poe, R. H. (2008). Chest imaging techniques and indications. In J. E. Fishman, A. S. Elias, & J. R. Rubinowitz (Eds.), *Chest medicine: Essentials of pulmonary and critical care* (5th ed., pp. 95-110). Lippincott Williams & Wilkins.

Rosa, M. E., & Hellinger, W. C. (2018). Radiologic diagnosis of lung infections: A focus on viral pneumonia. *Radiologic Clinics of North America, 56*(2), 271-283. https://doi.org/10.1016/j.rcl.2017.09.009

Umme Sara, Rahman, S. H., Akter, S., & Mita, N. A. (2019). A survey on the application of machine learning techniques for breast cancer diagnosis. *Journal of Computer and Communications, 7*(1), 12-19. https://doi.org/10.4236/jcc.2019.71002